Available online www.jocpr.com

Journal of Chemical and Pharmaceutical Research, 2013, 5(7):56-69

Research Article

ISSN : 0975-7384
CODEN(USA) : JCPRC5

Synthesis, characterization and biological studies of Cu(II), Co(II), Ni(II) and Zn(II) complexes of tetradentate Schiff base ligand

J. Senthil Kumaran[a], S. Priya[a], J. Muthukumaran[b], N. Jayachandramani and S. Mahalakshmi[a*]

[a] *PG & Research Department of Chemistry, Pachaiyappa's College, Chennai*
[b] *Centre for Bioinformatics, School of Life Sciences, Pondicherry University, Puducherry*

ABSTRACT

A novel series of transition metal complexes of Cu(II), Co(II), Ni(II) and Zn(II) derived from 2-hydroxy-3-formylquinoline, 4-aminoantipyrine and 2-aminothiazole were synthesized and characterized by IR, ^{1}H NMR, UV-Vis., ESR and Mass spectra. IR spectral studies show the binding sites of the Schiff base ligand with the metal ion. Molar conductance data and magnetic susceptibility measurements give evidence for monomeric and neutral nature of the complexes. The electrochemical behaviour of the copper complex at room temperature (RT) was studied. The X band ESR spectrum of the Cu(II) complex at RT and liquid nitrogen temperature (LNT) was recorded. The in silico DNA results reveal that copper complex is bound to the "Minor groove and cobalt, nickel and zinc complexes are bound to the "Major groove" portion of DNA through hydrogen bonds and hence they are called "Minor groove and Major groove binders" respectively. The in vitro biological activities of the ligand and its complexes were tested against pathogenic bacterial species Escherichia coli, Pseudomonas aeruginosa, Bacillus subtilis and Staphylococcus aureus and fungal species Candida albicans.

Key words: 4-aminoantipyrine, 2-hydroxy-3-formylquinoline, Schiff base, *in silico* DNA study, antimicrobial activity

---

INTRODUCTION

The Schiff bases are widely used ligands due to their facile synthesis, significant versatility and good solubility in common solvents. Thus, they have played a vital role in the development of coordination chemistry as they readily form stable complexes with most metals in different oxidation states [1]. In Schiff bases, the azomethine linkage is an important for biological activity; several azomethines were reported to possess significant antibacterial [2-4], antifungal [5, 6], anticancer [7], and diuretic activities [8]. Quinoline and its derivatives, naturally occurring antibiotic, are one of the most widely used as antibacterial, anticonvulsant and antimalarial drugs [9-13]. In recent decades, a great deal of interest in the metal complexes of nitrogen–oxygen chelating agents derived from 4-aminoantipyrine Schiff bases have various applications in antifungal, antibacterial [14], analgesic, sedative, antipyretic, anti-inflammatory [15] and greater DNA binding ability [16]. Thiazoles have a broad range of antitumor, antibiotic, antibacterial, antifungal and anti-inflammatory activities [17-20]. The present work deals with the synthesis, characterization, *in silico* DNA studies and antimicrobial evaluation of the Schiff base derived from 2-hydroxy-3-formylquinoline, 4-aminoantipyrine and 2-aminothiazole and its Cu (II), Co(II), Ni(II) and Zn(II) complexes.

EXPERIMENTAL SECTION

2.1 Experimental

2.1. Materials and Methods

2-hydroxy-3-formylquinoline was synthesized by the method reported earlier [21]. 4-Aminoantipyrine and 2-aminothiazole were obtained from Sigma. Metal chlorides were purchased from Merck. All chemicals used were of AR grade. Solvents were purified and distilled before use. Molar conductivity was determined using Systronic Conductivity Bridge with a dip type cell 783 spectrometer in the range 4000-400 cm^{-1}. UV-Visible spectra of the complexes were recorded on Perkin Elmer Lambda EZ201 spectrophotometer in DMSO solution. ^1H NMR spectra were recorded on a Bruker 300 MHz instrument using $CDCl_3$ as a solvent and TMS as an internal standard. The RT magnetic measurements were carried out using Guoy balance and the diamagnetic corrections were made using Pascal's constant. FAB-MS spectra were recorded with a VGZABHS spectrometer at RT in a 3-nitrobenzylalcohol matrix. Cyclic Voltammetry studies were performed on a CHI 760C electrochemical analyzer in single compartmental cells at RT using tetrabutylammonium perchlorate (TBAP) as a supporting electrolyte. X-band EPR spectra of the copper complexes were recorded in DMSO at RT and LNT at Sophisticated Analytical Instrument Facility (SAIF), IIT, Mumbai.

2.2 Synthesis of Schiff base ligand

The Schiff base ligand was synthesized by two methods as given below.

Method 1

4-aminoantipyrine-2-aminothiazole was synthesized by the method reported earlier [22]. 2-Hydroxy-3-formylquinoline (0.01 mol) and 4-aminoantipyrine-2-aminothiazole (0.01 mol) were dissolved in hot ethanol. A few drops of acetic acid were added and the solution was refluxed for 10 h with continuous stirring. The Schiff base product formed was filtered and recrystallized from ethanol (**Scheme 1**) (Yield: 68%).

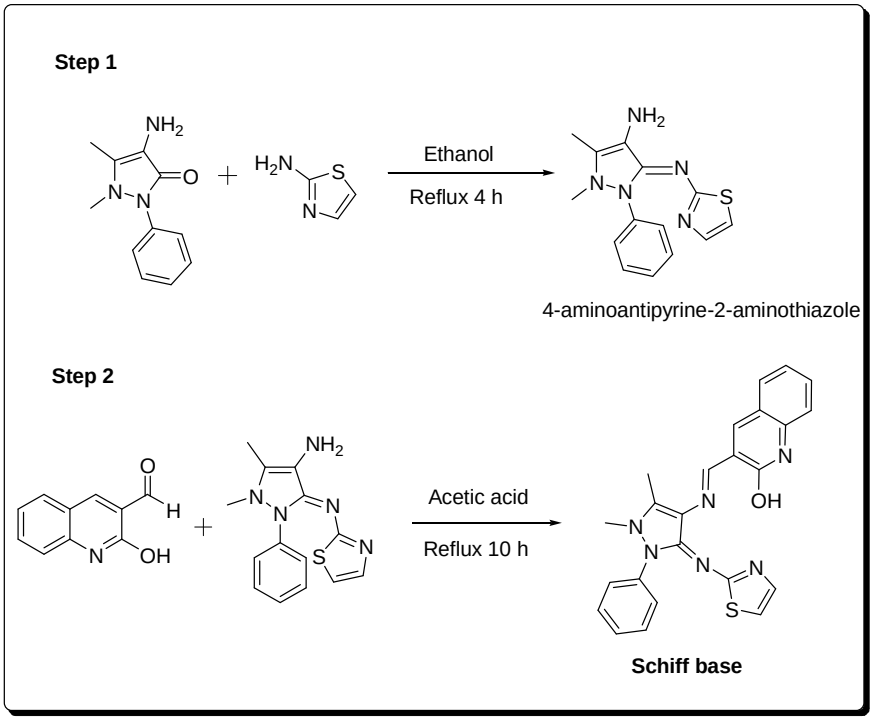

Scheme 1. Synthesis of Schiff base ligand by method 1

Method 2

4-hydroxy-3-methoxybenzylidine-4-aminoantipyrine was synthesized by the condensation of 4-hydroxy-3-methoxybenzaldehyde and 4-aminoantipyrine as reported earlier [13]. 4-hydroxy-3-methoxybenzylidine-4-

aminoantipyrine (0.01 mol) and 2-aminthiazole (0.01 mmol) were taken in ethanol. To this mixture, 1 g of anhydrous potassium carbonate was added and then refluxed for 10 hrs. The resulting solution was concentrated on a water bath and allowed to cool at 0°C for ~24 h. The solid product formed was separated by filtration and washed thoroughly with ethanol and then dried *in vacuum* (**Scheme 2**) (Yield: 60%). Of these two methods the first one gave a better yield of the ligand.

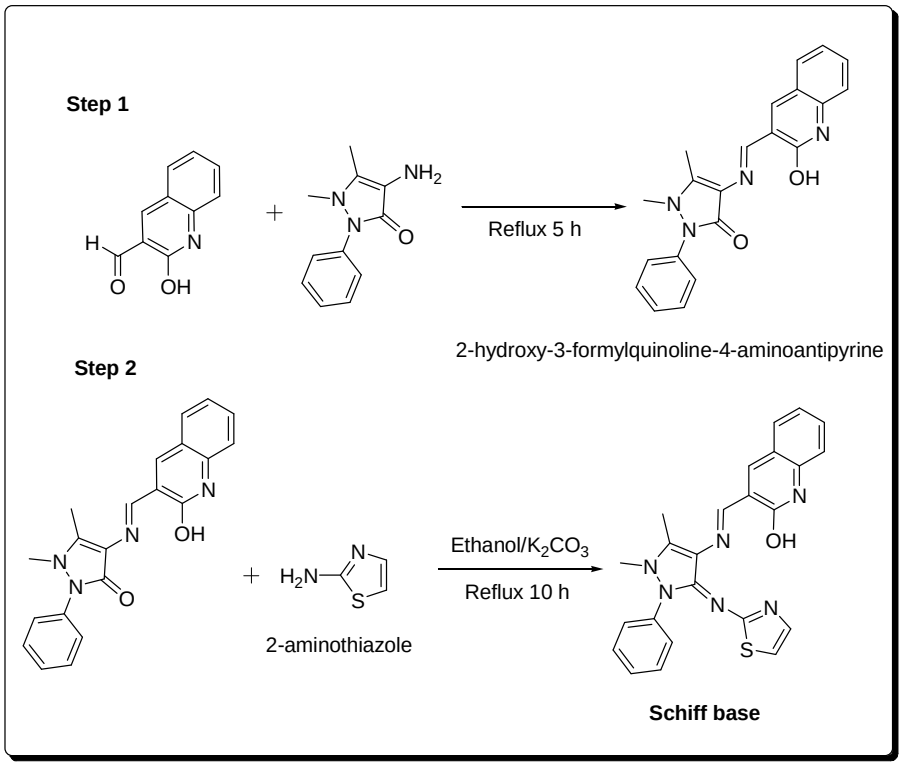

Scheme 2. Synthesis of Schiff base ligand by method 2

2.3 Synthesis of metal complexes

Equimolar amounts of Schiff base ligand and metal chloride were refluxed with hot ethanolic solution (50 mL) for about 2 h. Then the solution was concentrated to one third of volume on a water bath. The solid complex precipitated was filtered off and washed thoroughly with ethanol and dried in *vacuo*.

2.3 In silico studies on DNA and metal complexes

DNA with metal complex interaction was studied by molecular modeling with special reference to docking**.** The crystal structure of the complex of netropsin with B-DNA dodecamer d(CGCGAATTCGCG)2 (NDB code GDLB05) was downloaded from Protein Data Bank. Crystallographic water molecules were removed from the DNA. On the basis of literature evidences [23, 24], we have selected the DNA sequence and it was subjected to DNA sequence to structure web server [25] for generating the three-dimensional structure of DNA based on experimental fiber-diffraction studies [26]. Metal complexes structure was drawn using ChemDraw Ultra10.0 program and three-dimensional structure of metal complexes was prepared by using Discovery studio 3.1 [27]. The DNA-metal complex interaction was studied using Patch dock web server [28]. The PyMol stand-alone program [29] was used to visualize the interaction between DNA structure and metal complexes. HBAT [30], the hydrogen bond analysis tool was used to analyze the hydrogen bonds present between DNA and metal complexes. In this in-house developed program, the standard hydrogen bond distance (H…A) and angle (X-H…A) was set as 2.8 Å and 90º, respectively.

2.4. Biological Activity

The biological evaluation of synthesized Schiff Base and its Cu(II), Co(II), Ni(II), and Zn(II) complexes have been studied for their antibacterial and antifungal activities by *well diffusion* test using Mueller-Hinton Agar (MHA) and

Sabouraud Dextrose Agar (SDA). Stock solutions of all compounds were diluted with dimethyl sulfoxide. The stock solutions were prepared for 3 mg of Compound/2 mL of DMSO concentration. From the stock solution, different diluted measurements such as 20 μL, 40 μL 60 μL (20 μL diluted sample contains 30 μg of the test compound) were immediately dispensed into agar wells of culture inoculated plates (MHA) using sterilized microchips. The plates were incubated at 37°C overnight. The antimicrobial activity was measured as the diameter of the inhibition zone including the diameter of the well.

RESULTS AND DISCUSSION

3.1 Elemental analysis and molar conductivity measurements

The analytical data for the ligand and complexes together with some physical properties are summarized in **Table 1**. The analytical data of the complexes correspond well with the general formula MLCl, where M = Cu(II), Co(II), Ni(II) and Zn(II); L = $C_{24}H_{19}N_6OS$. The magnetic susceptibilities of the complexes at RT are consistent with square-planar geometry around the central metal ion.

The formation of these complexes may proceed according to the equation given below:

$MCl_2.nH_2O + L \rightarrow MLCl + HCl + nH_2O$
Where, M = Cu(II), Co(II), Ni(II) and Zn(II)

The metal(II) complexes were dissolved in DMSO and the molar conductivities of 10^{-3}M solutions at RT were measured. The higher conductance values (128–148 Ω^{-1} cm^2 mol^{-1}) of the complexes indicate their electrolytic nature [31].

3.2 Mass spectra

The mass spectra of the ligand and its copper and zinc complexes were recorded and compared for their stoichiometric compositions. The molecular ion peak for the ligand is observed at 440 m/z ratio. The molecular ion peak for the copper complex was observed at m/z 538, which confirms the stoichiometry of copper complex as MLCl type. It is also supported by the mass spectra of zinc complex, M+1 peak appeared at m/z 541. Microanalytical data are also in close agreement with the values calculated from molecular formula assigned to these complexes.

3.3 Infrared Spectra

The IR spectra give valuable information regarding the nature of the functional group attached to the metal ion. The IR spectral data of the Schiff base and its complexes are given in **Table 2.** The IR spectrum of the ligand dissplays a broad band in the region 3200-3600 cm^{-1}, assignable to $\upsilon_{(OH)}$ group. The disappearance of this peak in all the spectra of the complexes indicate that the –OH group is involved in complexation. The spectrum of the ligand shows two different $\upsilon_{(C=N)}$ bands in the region 1615-1690 cm^{-1}, which are shifted to lower frequencies in the spectra of all the complexes (1600-1650 cm^{-1}) indicating the involvement of –C=N nitrogen in coordination to the metal ion [32-33]. Also the ligand shows a band at 1610 cm^{-1} which is attributed to $\upsilon_{(CH=N)}$ of thiazole ring and $\upsilon_{(C=C)}$ at 1552 cm^{-1}. The stretching vibration appearing at 785 cm^{-1} is due to $\upsilon_{(C-S)}$ of thiazole ring [15]. A shift in the band at 1610 cm^{-1} of the thiazole ring (1600–1580 cm^{-1}) in complexes suggest the coordination via thiazole nitrogen (N → M) [34]. In all the complexes the $\upsilon_{(C-S)}$ remains unchanged indicating that sulphur is not involved in the coordination. IR spectra of complexes show new bands at 444–488 cm^{-1} and 528–568 cm^{-1} assignable to υ(M–N) and υ(M–O) modes respectively [35].

3.4 ^{1}H-NMR spectra

^{1}H NMR spectra of the Schiff base ligand and its zinc complex were recorded at RT in $CDCl_3$. Schiff base ligand (HL) exhibited the following signals: aromatic protons at 7.14-7.40 δ (10H, m), -CH=N at 9.76 δ (1H, s), -N-CH_3 at 3.08 δ (3H, s), C-CH_3 at 2.44 δ (3H, s) and S-CH=CH- of thiazole ring at 7.74 δ (1H, d). N-CH=CH of thiazole proton of free ligand at 7.86 δ (1H, d) also showed a downfield shift in the complex providing an evidence of coordination of thiazole nitrogen to the metal. The peak at 12.14 δ is attributable to –OH of quinoline moiety observed in Schiff base. The absence of this peak noted for zinc complex indicates the loss of the OH proton due to chelation. The azomethine proton signals in the spectra of zinc complexes were moved to downfield compared to the Schiff base ligand, suggesting deshielding of azomethine group due to coordination with metal atom. There is no

significant change in all other signals of the ligand. ^{1}H-NMR spectra of Schiff base ligand and its zinc complex are given in **Figure 1-2.**

3.5 Electronic absorption spectroscopy

The electronic absorption spectra were recorded at 300 K. The various absorptions, band assignments and the proposed geometry of the complexes are given in **Table 3.** The electronic spectra of copper complex displays two bands, which are assigned as an intra-ligand charge transfer band (31,446 cm^{-1}) and d-d band (19,685 cm^{-1}) which is due to $^2B_{1g}\rightarrow{}^2A_{1g}$ transition. This d-d band strongly favors square-planar geometry for the copper complex [36-38]. It is further supported by its magnetic susceptibility value (1.73 B.M) [39]. The UV-visible spectrum of Cobalt(II) complex shows two peaks at 28,409 cm^{-1} and 22,421 cm^{-1}. The first peak is due to intraligand charge transfer band and the band at 22,421 cm^{-1} is due to the $^1A_{1g}\rightarrow{}^1B_{1g}$ transition. This is true of square-planar geometry. This is further confirmed by its magnetic susceptibility value (3.52 B.M). Nickel(II) has a (d^8) configuration giving peaks at 27,932 cm^{-1} and 22,988 cm^{-1}. The first peak is assigned to the intraligand charge transfer band and the second peak is for $^1A_{1g} \rightarrow {}^1B_{1g}$ for square planar geometry [40]. No transitions were observed in the visible region for Zn(II) complex consistent with the d^{10} configuration of the Zn(II) ion. This complex is also found to be diamagnetic in nature and as expected for d^{10} configuration. According to stoichiometry of these complexes and elemental analyses they are four coordinated, which could be a square-planar geometry.

3.6 Cyclic Voltammetry

The electrochemical behavior of Schiff base copper complex has been examined by cyclic voltammetry. Tetrabutylammoniumperchlorate (TBAP) was used as supporting electrolyte. The cyclic voltammogram of the copper complex in DMSO (scan rate 100 mVs^{-1}) shows a well-defined redox process corresponding to the formation of Cu(II)/Cu(I) couple at E_{pa} = -0.056 V and the associated cathodic peak at E_{pc} = −0.121 V. This couple is found to be quasi-reversible with ΔE_p = 0.177 V and the ratio of anodic to cathodic peak currents corresponding to a simple one-electron process [41].

3.7 Electron paramagnetic resonance spectra

The ESR spectra of the copper complex, recorded in DMSO solution at 300 and 77 K are shown in **Figure 3-4.** The frozen solution (LNT) spectrum shows a well resolved four line spectrum and no features characteristic for a dinuclear complex. This is also indicated by the magnetic moment of copper complex (1.73 B.M) which confirms the mononuclear nature of the complex. The spin Hamiltonian parameters for the copper complex were calculated from the spectra. The g-tensor values of this copper(II) complex can be used to derive the ground state. In square-planar complexes, the unpaired electron lies in the $d_{x^2-y^2}$ orbital, giving $^2B_{1g}$ as the ground state with $g_{\|} > g_{(} > 2$, while the unpaired electron lies in the d_{z^2} orbital, giving $^2A_{1g}$ as the ground state with $g_{(} > g_{\|} > 2$. From the experimental values, it is clear that $g_{\|}$ (2.18) > $g_{\perp}$ (2.03) > 2, which suggests that the complex is square planar. This is further supported by the fact that the unpaired electron lies predominantly in the $d_{x^2-y^2}$ orbital [42-45], as was evident from the value of the exchange interaction term G, estimated from the expression: $G = (g_{\|} - 2.00277)/(g_{\perp} - 2.00277)$.

If G > 4.0, the local tetragonal axes are aligned parallel or only slightly misaligned. If G < 4.0, significant exchange coupling is present and the misalignment is appreciable. The experimental value for the exchange interaction parameter for the copper complex (G = 6.5) suggests that the local tetragonal axes are aligned parallel or slightly misaligned and that the unpaired electron is present in the $d_{x^2-y^2}$ orbital. This result also shows that the exchange coupling effects are not operative in the complex [46].

Based on the above spectral and analytical data, the proposed geometry of the metal(II) complexes is given in **Figure 5**.

3.8 In silico DNA-metal complex interaction

The Patch dock web server was used to study the interaction between DNA and metal complexes. For each docking results, the best solution was inferred by highest value of shape complementarity score **(Table 4)**. The shape-complementarity score of the four complexes was computed using Patch dock web server. From the molecular docking results **(Figure 6)**, the best solution was selected and it was processed into Hydrogen Bond Analysis Tool (HBAT) for computing the possible inter-molecular hydrogen bonds present between DNA and metal complexes. HBAT results revealed that two inter-molecular C-H…O and C-H…N hydrogen bonds played a vital role for the stability all the complexes with DNA. The details of inter-molecular C-H…O, C-H…N and C-H…S interactions

were given in **Tables 5-8**. However, Co(II), Cu(II) and Ni(II) complexes did not show other inter-molecular hydrogen bonds such as N-H…O, O-H…O, N-H…N, O-H…N, N-H...S, O-H...S, C-H...S, C-H… π, N-H… π and O-H… π. Zn(II) complex exhibits C-H…O, C-H…N and C-H…S interactions. **Figure 7** and **Table 9** gives the statistics of various possible inter-molecular hydrogen bonds present between DNA and metal complexes.

Patch dock and HBAT analysis results propose that the via hydrogen bonding cobalt, nickel and zinc complexes are bound to the "Minor groove" portion of DNA and hence they are called "Minor groove binders" and copper complex is bound to "Major groove" portion and called "Major groove binders".

3.9 Antimicrobial activity

The Schiff base ligand and its metal complexes have been monitored for their antibacterial activities against various pathogenic bacteria such as *Escherichia coli*, *Pseudomonas aeruginosa*, *Bacillus subtilis*, *Staphylococcus aureus* and fungal activity against *Candida albicans. Tetracycline* and *amphotericin* were used as the standard for bacterial and fungal studies respectively. The antimicrobial activity of the Schiff base and its complexes were tested against human pathogenic bacterias and the zones of inhibition are given in **Table 10.** A comparative study of the growth inhibition zone values of Schiff base and its complexes show that metal complexes display higher antibacterial activity than the free ligand and this is probably due to the greater lipophilic nature [47-49] of the complexes. Metal complexes activity can be explained on the basis of Overtone's concept [50] and Tweedy's chelation theory [51].

Table 1 Physical and analytical data of the synthesized Schiff base and its complexes

Compound	Empirical Formula	Yield (%)	Colour	Found (Calculated) (%)				Formula weight	($\wedge_M$) $\Omega^{-1}cm^2$ mol^{-1}	μ_{eff} (B.M.)
				M	C	H	N			
Schiff base (HL)	$C_{24}H_{20}N_6OS$	68	Brown	-	65.26 (65.44)	4.24 (4.58)	19.25 (19.08)	440.5	-	-
[CuL] Cl	$[CuC_{24}H_{19}N_6OS]$ Cl	58	Black	11.66 (11.80)	53.89 (53.53)	3.14 (3.56)	15.17 (15.61)	538.5	128	1.73
[CoL] Cl	$[CoC_{24}H_{19}N_6OS]$ Cl	54	Red	11.22 (11.04)	53.42 (53.99)	3.37 (3.59)	15.34 (15.74)	533.8	130	3.52
[NiL] Cl	$[NiC_{24}H_{19}N_6OS]$ Cl	62	Green	11.14 (11.00)	54.35 (54.02)	3.25 (3.59)	15.05 (15.75)	533.6	135	Diamagnetic
[ZnL] Cl	$[ZnC_{24}H_{19}N_6OS]$ Cl	44	Brown	11.87 (12.10)	53.20 (53.35)	3.99 (3.54)	15.17 (15.55)	540.3	148	Diamagnetic

Table 2 The IR spectral data of Schiff base and its complexes (cm^{-1})

Compound	$\upsilon_{(OH)}$	$\upsilon_{(C-S)}$	$\upsilon_{(C=N)}$	$\upsilon_{(M-N)}$	$\upsilon_{(M-O)}$
Schiff base (HL)	3439	785	1645, 1688	-	-
[CuL] Cl	-	788	1622, 1638	488	528
[CoL] Cl	-	782	1618, 1645	444	530
[NiL] Cl	-	786	1615, 1627	485	533
[ZnL] Cl	-	780	1629, 1642	472	568

Table 3 Electronic spectral data of Schiff base and its complexes

Compound	Absorption nm (cm^{-1})	Band assignments	Geometry
Ligand (HL)	364 (27,472)	INCT	-
[CuL] Cl	318 (31,446) 508 (19,685)	INCT $^2B_{1g} \rightarrow {}^2A_{1g}$ transition	Square planar
[CoL] Cl	352 (28,409) 445 (22,421)	INCT $^1A_{1g} \rightarrow {}^1B_{1g}$ transition	Square planar
[NiL] Cl	358 (27,932) 435 (22,988)	INCT $^1A_{1g} \rightarrow {}^1B_{1g}$ transition	Square planar

INCT=Intraligand charge transfer band.

Table 4 Shape complementarity score of DNA-Metal complexes

S. No	Metal Complex	Shape-Complementarity Score
1.	DNA – [CoL] Cl	4306
2.	DNA – [CuL] Cl	4390
3.	DNA – [NiL] Cl	4484
4.	DNA – [ZnL] Cl	4394

Table 5 Inter-molecular hydrogen bonds present in DNA-cobalt complex

Type	Donor	Donor Atom	Acceptor	Acceptor Atom	*d* (H···A) (Å)	*D* (X···A) (Å)	q (X−H···A) (º)
C-H...N	Adenine	C2	[CoL] Cl	N16	2.949	3.997	163.5
C-H...N	Cytosine	C4	[CoL] Cl	N2	2.021	3.038	153.9
C-H...O	Adenine	C2	[CoL] Cl	O24	2.582	3.523	145.1
C-H...N	Thymine	C4	[CoL] Cl	N3	2.976	3.711	124.9
C-H...N	Thymine	C1	[CoL] Cl	N10	1.690	2.070	93.72
C-H...O	Thymine	C1	[CoL] Cl	O24	2.885	3.367	106.8
C-H...N	Thymine	C1	[CoL] Cl	N5	2.173	2.875	125.8
C-H...O	Thymine	C1	[CoL] Cl	O24	2.842	3.367	113.3
C-H...O	Thymine	O4	[CoL] Cl	O24	2.842	3.073	98.15
C-H...N	[CoL] Cl	C6	Thymine	N1	1.574	2.584	151.3
C-H...O	[CoL] Cl	C6	Thymine	O2	2.706	3.527	131.7
C-H...O	[CoL] Cl	C8	Thymine	O1P	2.204	3.017	129.4
C-H...O	[CoL] Cl	C8	Thymine	O2P	2.062	3.026	145.7
C-H...O	[CoL] Cl	C8	Thymine	O5	2.830	3.297	105.7
C-H...O	[CoL] Cl	C9	Thymine	O1P	2.461	3.170	121.4
C-H...O	[CoL] Cl	C9	Thymine	O5	2.554	2.906	97.54
C-H...N	[CoL] Cl	C23	Adenine	N3	2.926	3.945	157.4
C-H...O	[CoL] Cl	C27	Adenine	O3	2.988	3.305	97.34
C-H...O	[CoL] Cl	C27	Thymine	O5	2.719	3.629	141.6
C-H...O	[CoL] Cl	C28	Adenine	O3	1.846	2.798	144.6
C-H...O	[CoL] Cl	C30	Guanine	O4	2.884	3.856	149.7
C-H...O	[CoL] Cl	C31	Cytosine	O4	2.493	3.462	148.7
C-H...O	[CoL] Cl	C32	Cytosine	O3	2.124	2.972	132.5

Table 6 Inter-molecular hydrogen bonds present in DNA-copper complex

Type	Donor	Donor Atom	Acceptor	Acceptor Atom	*d* (H···A) (Å)	*D* (X···A) (Å)	q (X−H···A) (º)
C-H…N	[CuL] Cl	C8	Adenine	N6	20606	3.232	115.7
C-H…O	[CuL] Cl	C9	Thymine	O4	2.800	3.888	177.2
C-H…O	[CuL] Cl	C19	Thymine	O2P	2.153	2.858	120.5
C-H…O	[CuL] Cl	C20	Adenine	O3	2.628	3.589	147.9
C-H…O	[CuL] Cl	C20	Thymine	O2P	1.419	2.369	142.3
C-H…O	[CuL] Cl	C21	Adenine	O1P	2.213	2.552	95.33
C-H…O	[CuL] Cl	C21	Adenine	O5	2.991	3.202	91.19
C-H…O	[CuL] Cl	C22	Adenine	O1P	1.942	2.422	102.7
C-H…O	[CuL] Cl	C28	Guanine	O2P	2.175	3.213	160.0
C-H…O	[CuL] Cl	C29	Cytosine	O1P	2.300	3.254	146.2
C-H…O	[CuL] Cl	C29	Cytosine	O5	2.111	2.698	111.2
C-H…O	[CuL] Cl	C30	Cytosine	O2P	1.059	1.981	135.7
C-H…N	[CuL] Cl	C32	Cytosine	N4	2.763	3.540	127.9
C-H…O	[CuL] Cl	C32	Guanine	O6	2.872	3.837	147.4
C-H…O	[CuL] Cl	C33	Thymine	O4	2.821	3.735	141.3

Table 7 Inter-molecular hydrogen bonds present in DNA-nickel complex

Type	Donor	Donor Atom	Acceptor	Acceptor Atom	*d* (H···A) (Å)	*D* (X···A) (Å)	q (X−H···A) (º)
C-H...O	Thymine	C4	[NiL] Cl	O24	2.970	3.752	128.8
C-H...N	Thymine	C4	[NiL] Cl	N16	2.092	2.537	100.9
C-H...N	Cytosine	C4	[NiL] Cl	N12	2.723	3.510	128.7
C-H...O	[NiL] Cl	C9	Cytosine	O3	2.997	3.623	116.8
C-H...O	[NiL] Cl	C13	Thymine	O2	2.847	3.781	144.8
C-H...O	[NiL] Cl	C19	Thymine	O4	2.367	3.001	115.8
C-H...O	[NiL] Cl	C20	Thymine	O2	2.192	3.091	139.3
C-H...O	[NiL] Cl	C20	Thymine	O4	2.554	3.188	116.6
C-H...O	[NiL] Cl	C21	Thymine	O4	2.803	3.701	140.4
C-H...O	[NiL] Cl	C23	Thymine	O3	2.319	3.338	156.4
C-H...O	[NiL] Cl	C30	Thymine	O1P	2.627	3.003	99.59
C-H...O	[NiL] Cl	C31	Adenine	O3	2.373	3.220	134.0
C-H...O	[NiL] Cl	C33	Cytosine	O4	2.248	2.858	113.0
C-H...O	[NiL] Cl	C33	Cytosine	O4	2.620	2.858	91.10

Table 8 Inter-molecular hydrogen bonds present in DNA-zinc complex

Type	Donor	Donor Atom	Acceptor	Acceptor Atom	*d* (H···A) (Å)	*D* (X···A) (Å)	q (X−H···A) (º)
C-H…N	Thymine	C4	[ZnL] Cl	N12	2.793	3.457	119.0
C-H…N	Cytosine	C4	[ZnL] Cl	N3	1.282	1.957	110.8
C-H…N	Thymine	C4	[ZnL] Cl	N5	2.555	3.350	128.9
C-H…S	Thymine	C4	[ZnL] Cl	S7	1.302	2.245	139.2
C-H…N	Thymine	C4	[ZnL] Cl	N10	2.879	3.488	115.3
C-H…N	Thymine	O4	[ZnL] Cl	N5	2.172	3.129	139.2
C-H…S	Thymine	O4	[ZnL] Cl	S7	2.473	3.183	118.5
C-H…O	[ZnL] Cl	C6	Thymine	O4	1.143	2.195	159.1
C-H…O	[ZnL] Cl	C13	Thymine	O3	2.484	3.326	133.9
C-H…O	[ZnL] Cl	C22	Cytosine	O4	2.687	3.340	118.4
C-H…O	[ZnL] Cl	C23	Thymine	O2	2.107	2.954	133.1
C-H…O	[ZnL] Cl	C30	Cytosine	O2	1.965	2.677	120.1
C-H…O	[ZnL] Cl	C30	Guanine	O4	2.247	3.046	129.0
C-H…N	Cytosine	C1	[ZnL] Cl	N2	2.844	3.201	94.45
C-H…N	Cytosine	C1	[ZnL] Cl	N3	2.644	3.504	123.5
C-H…O	[ZnL] Cl	C31	Cytosine	O4	0.915	1.663	112.5
C-H…N	[ZnL] Cl	C31	Cytosine	N1	2.170	3.176	153.8
C-H…O	[ZnL] Cl	C31	Cytosine	O2	2.592	2.960	98.98
C-H…N	Cytosine	C3	[ZnL] Cl	N3	2.695	3.333	118.0
C-H…O	[ZnL] Cl	C32	Cytosine	O4	1.660	2.139	100.0
C-H…O	[ZnL] Cl	C32	Guanine	O5	2.980	3.875	139.5
C-H…N	Cytosine	C3	[ZnL] Cl	N2	2.096	2.308	91.11
C-H…O	[ZnL] Cl	C32	Cytosine	O5	2.058	2.807	123.1
C-H…O	[ZnL] Cl	C33	Cytosine	O1P	1.564	2.223	112.4
C-H…O	[ZnL] Cl	C33	Cytosine	O5	1.534	2.247	116.6
C-H…O	[ZnL] Cl	C33	Thymine	O3	1.392	2.250	129.7

Table 9 Statistics of inter-molecular hydrogen bonds present between DNA and metal complexes

Metal Complex	N-H…O	O-H…O	N-H…N	O-H…N	C-H…O	C-H…N	N-H…S	O-H…S	C-H…S
DNA – [CoL] Cl	0	0	0	0	16	7	0	0	0
DNA – [CuL] Cl	0	0	0	0	13	2	0	0	0
DNA – [NiL] Cl	0	0	0	0	12	2	0	0	0
DNA – [ZnL] Cl	0	0	0	0	14	10	0	0	2

Table 10Antimicrobial activity data for the Schiff base and its metal complexes

	E. coli			*P. aeruginosa*			*B. subtilis*			*S. aureus*			*C. albicans*		
Compound	30µg	60µg	90µL	30µg	60µg	90µg	30µg	60µg	90µg	30µg	60µg	90µg	30µg	60µg	90µg
Ligand (HL)	11	12	13	10	12	14	10	12	14	-	11	12	10	11	14
[CuL] Cl	13	18	23	16	21	22	13	15	17	10	12	13	14	18	20
[CoL] Cl	11	12	24	11	13	15	12	14	16	14	15	16	15	19	24
[NiL] Cl	13	16	18	12	13	14	13	15	17	10	12	13	10	14	18
[ZnL] Cl	19	23	26	12	13	14	15	17	21	16	17	21	14	18	20

Zone of Inhibition (mm)

Figure 1 ^{1}H-NMR spectra of Schiff base ligand

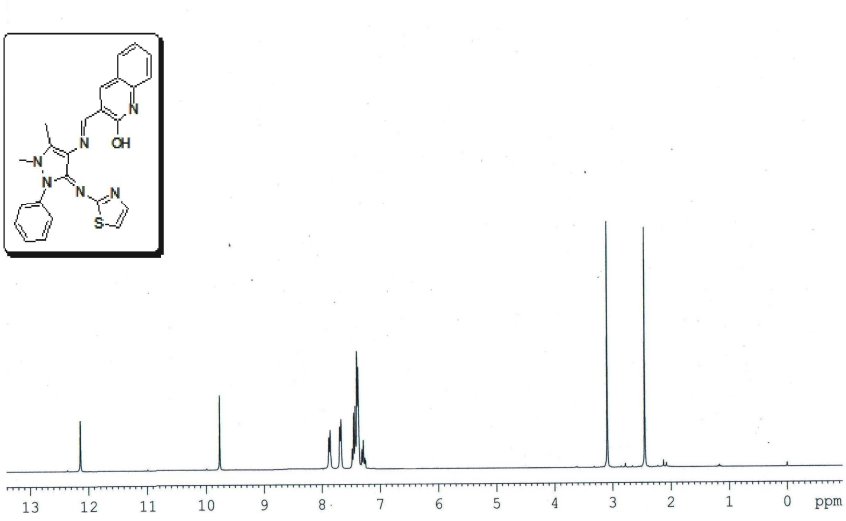

Figure 2 ^{1}H-NMR spectra of zinc complex

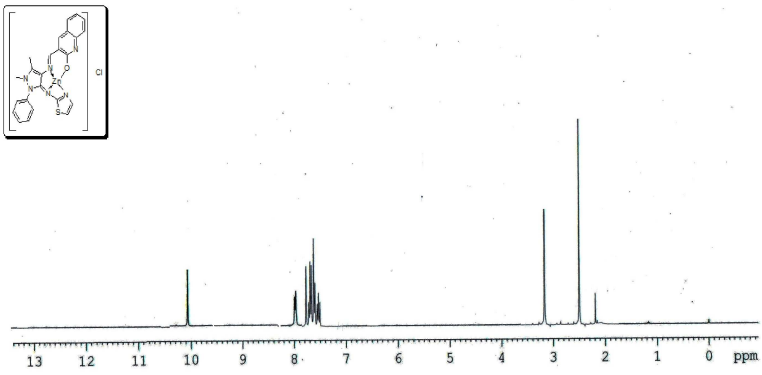

Figure 3 ESR spectra of copper complex at RT

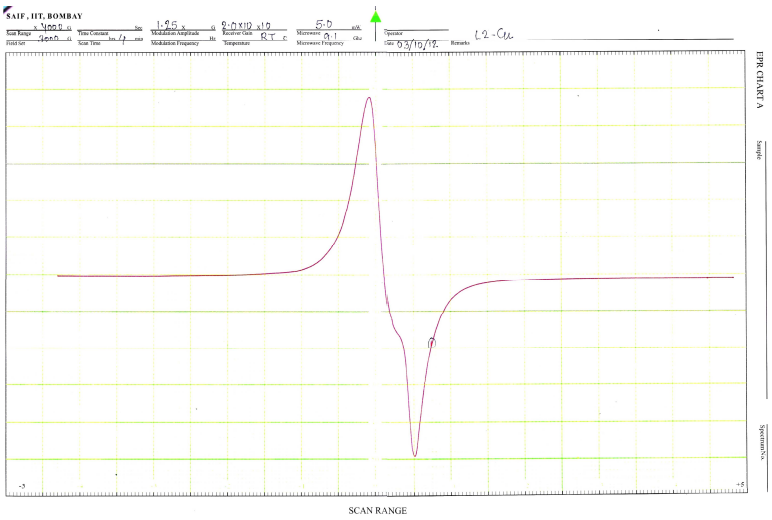

Figure 4 ESR spectra of copper complex at LNT

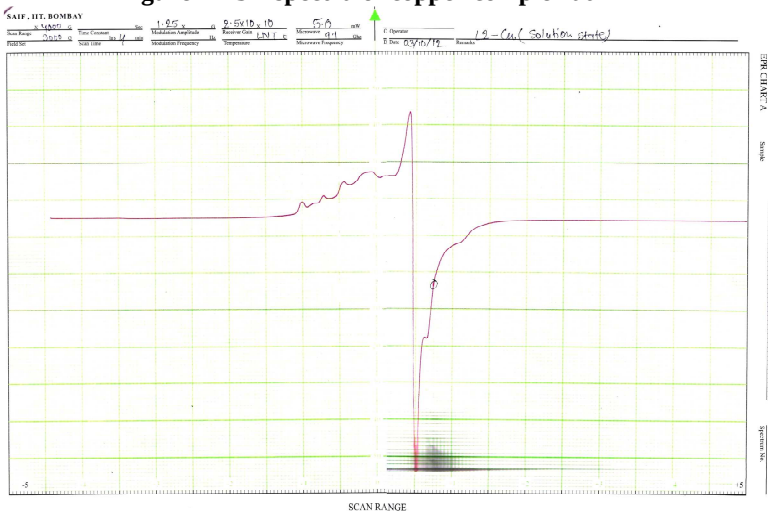

Figure 5 Square planar geometry of metal complexes, where M = Cu(II), Co(II), Ni(II) and Zn(II)

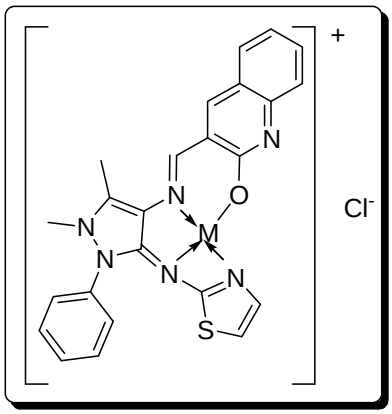

Figure 6 Molecular docking results of DNA–metal complex interaction (a) DNA-[CoL] Cl, (b) DNA-[CuL] Cl, (c) DNA-[NiL] Cl and (d) DNA-[ZnL] Cl complex. [Color codes: Ligand: Yellow, Representation: Stick, Display: PyMol]

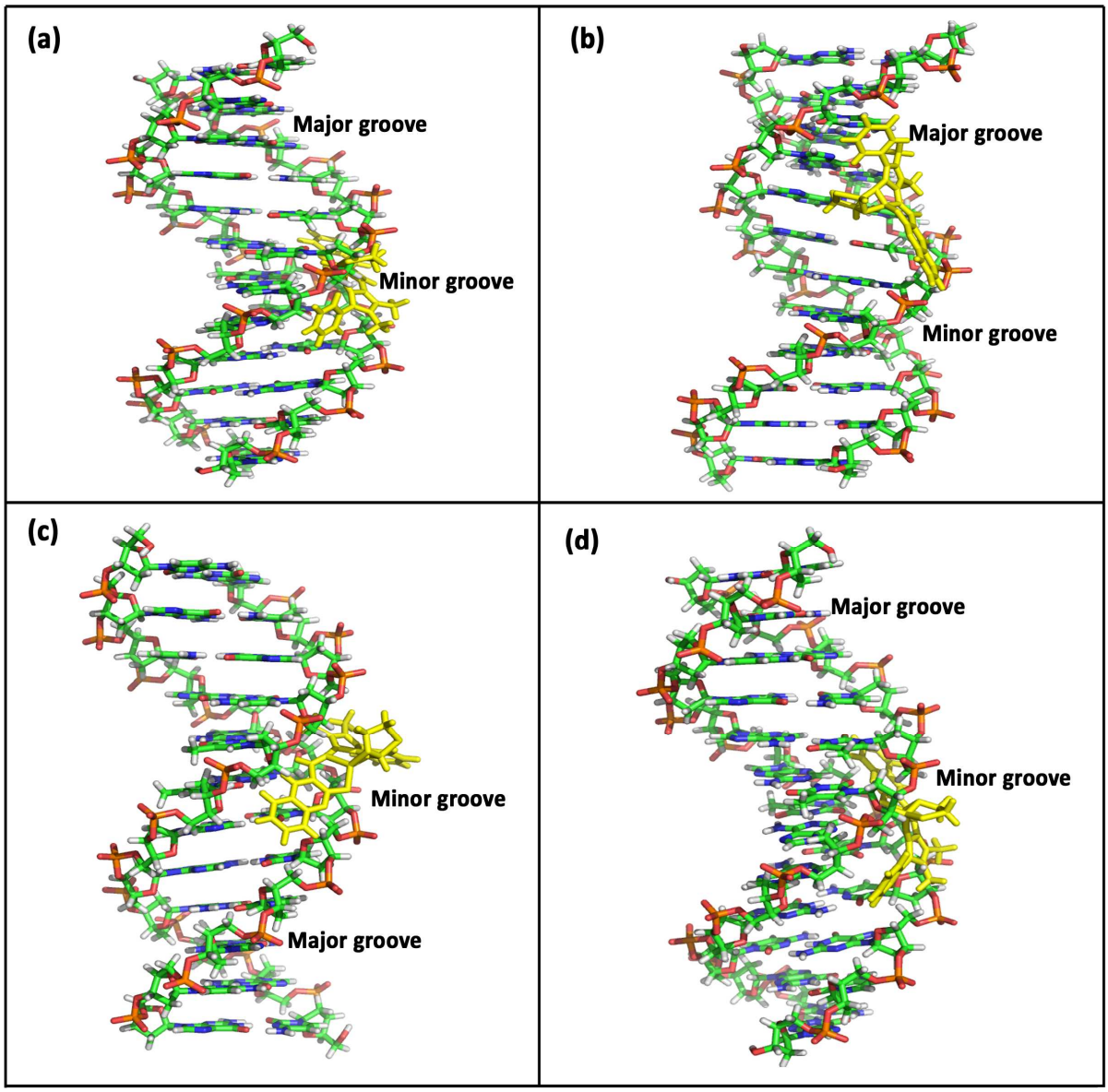

Figure 7 Statistics of various possible intermolecular hydrogen bonds present between DNA and metal complexes (a) DNA-[CoL] Cl, (b) DNA-[CuL] Cl, (c) DNA-[NiL] Cl and (d) DNA-[ZnL] Cl complex

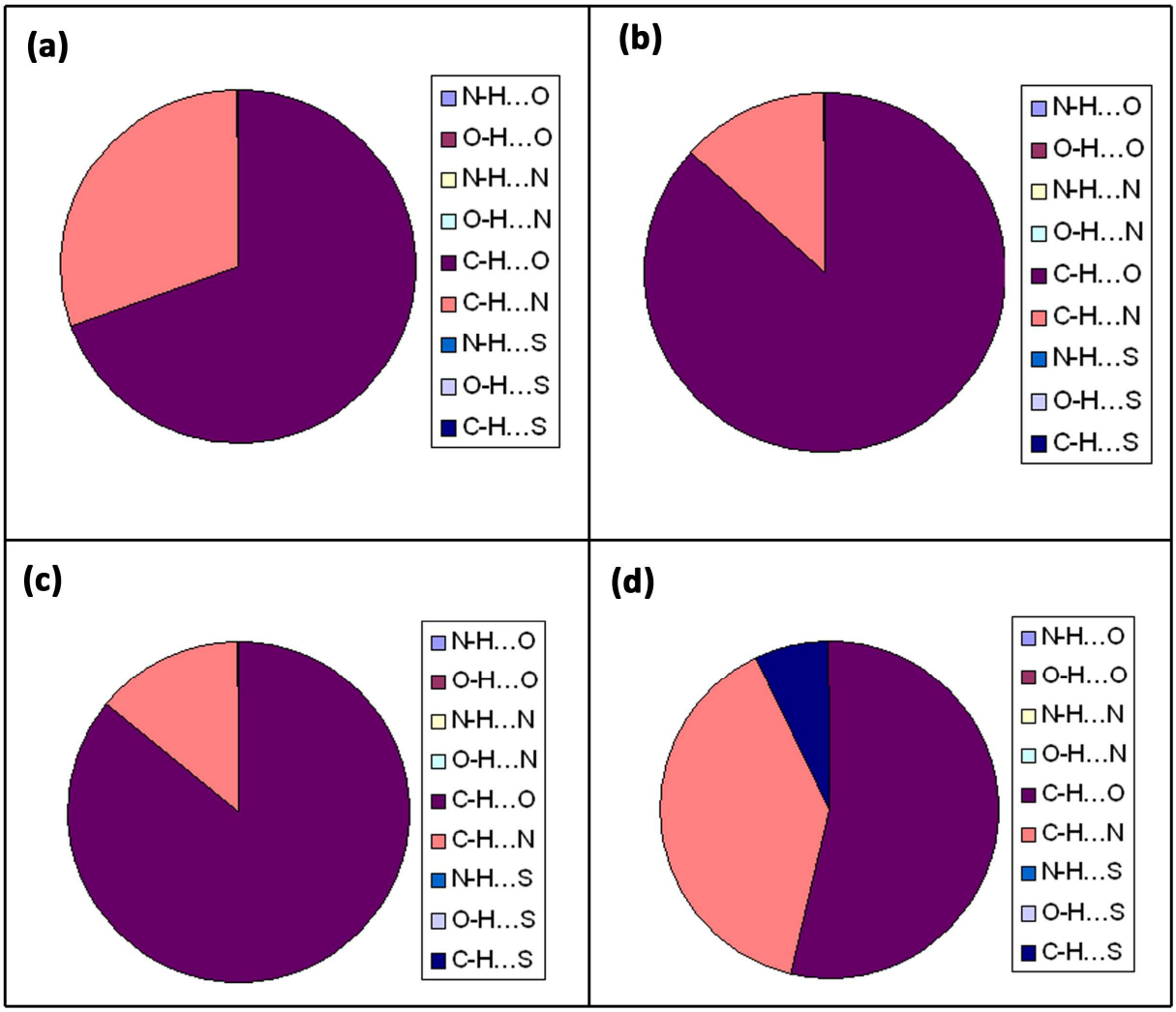

CONCLUSION

Cu(II), Co(II), Ni(II) and Zn(II) complexes with Schiff base derived from 2-hydroxy-3-formylquinoline, 4-aminoantipyrine and 2-aminobenzothiazole have been synthesized and characterized on the basis of elemental analyses, molar conductance, magnetic moment and spectral data. The Schiff base act as tetradentate ligand. All complexes show square planar geometry. The cyclic voltammogram of Cu(II) complex showed a well defined redox couple Cu(II)/Cu(I) with quasireversible nature. The interaction of these complexes with DNA was investigated by *in silico* method. From the observation, Co(II), Ni(II) and Zn(II) complexes interact with DNA through minor groove approach while Cu(II) interacts with DNA through major groove approach. Antibacterial and antifungal studies of the ligand and complexes have also been studied which indicate that activity increases on chelation.

Acknowledgements
The authors express their sincere to IIT, Bombay, India for ESR spectra. We are thankful to CDRI, Lucknow for elemental analyses.

REFERENCES

[1] KS Prasad; L Shiva Kumar; S Chandan; B Jayalakshmi; HD Revanasiddappaa. *Spectrochim. Acta, Part A*, **2011**, 81, 276-282.
[2] AK Bhendkar; K Vijay; AW Raut. *Acta Cienc. Indica, Chem.*, **2004,** 30, 29-32.
[3] YK Vaghasiya; R Nair; M Soni; S Baluja; S Chanda. *J. Serb. Chem. Soc*., **2004,** 69, 991-998.
[4] K Vashi; HB Naik. *Eur. J. Chem.*, **2004,** 1, 272-276.
[5] R Mtrei; M Yadawe; SA Patil, *Oriental Journal of Chemistry*, **1996**, 12, 101-102.
[6] ME Hossain; MN Allam; J Begum. *Inorg. Chim. Acta*, **1996,** 249, 207-213, 1996.
[7] VE Kuz'min; AG Artemenko; RN Lozytska. *SAR and QSAR in Environmental Research*, **2005,** 16, 219-230.
[8] CT Barboiu; M Luca; C Pop; E Brewster; ME Dinculescu. *Eur. J. Med. Chem.*, **1996,** 31, 597-606.
[9] Zeng-Chen Liu; Bao-Dui Wang; Bo Li; Qin Wang; Zheng-Yin Yang; Tian-Rong Li; Yong Li. *Eur. J. Med. Chem*. 45, 5353-5361.
[10] PD Duh; SC Wu; LW Chang; HL Chu; WJ Yen; BS Wang, *Food Chemistry*, **2009**, 114, 87-92.
[11] H Paritala; SM Firestine, *Bioorg. Med. Chem. Lett.*, **2009,** 19, 1584-1587.
[12] M Andaloussi; E Moreau; N Masurier; J Lacroix; RC Gaudreault. *Eur. J. Med. Chem.*, **2008,** 43, 2505-2517.
[13] GS Kurdekar; MP Sathisha; S Budagumpi; NV Kulkarni; VK Revankar; DK Suresh. *Med. Chem. Res.*, **2012,** 21, 2273-2279.
[14] GG Mohamed; MM Omar; A Ibrahim. *Eur. J. Med. Chem.*,**2009,** 44, 4801-4812.
[15] S Chandra; D Jain; AK Sharma; P Sharma. *Molecules*, **2009,** 14, 174-190.
[16] N Raman; N Selvan; P Manisankar. *Spectrochim. Acta, Part A*, **2010,** 76, 161-173.
[17] JG Michael; ML Tachel; LM Susanm; HB John; LB Milton. *Bioorg. Med. Chem.*, **2004,** 12, 1029-1036.
[18] AF Robert. *Clinical Microbiology Reviews*, **1988,** 1, 187-217.
[19] KY Jung; SK Kim; ZG Gao. *Bioorg. Med. Chem.*,**2004,** 12, 613-623.
[20] M Kalanithi; D Kodimunthiri; M Rajarajan; P Tharmaraj. *Spectrochim. Acta, Part A*, **2011,** 82, 290-298.
[21] P Nath; SD Dhumwad. *Journal of Chemical and Pharmaceutical Research*, **2012,** 4, 851-865.
[22] J Senthil Kumaran; S Priya; N; Jayachadramani; S Mahalakshmi. *Research Journal of Pharmaceutical Biological and Chemical Sciences*, **2013,** 4, 279-287.
[23] N Raman; S Sobha; A Thamaraichelvan. *Spectrochim. Acta, Part A*, **2010,** 78, 888-898.
[24] J Senthil Kumaran; S Priya; N Jayachandramani; S Mahalakshmi; *Journal of Chemistry*, 2013, 10 pages.
[25] http://www.scfbio-iitd.res.in/software/drugdesign/bdna.jsp .
[26] S Arnott; PJ Campbell-Smith; R Chandrasekaran. In Handbook of Biochemistry and Molecular Biology, 3rd ed. Nucleic Acids--**Volume II**, G.P. Fasman, Ed. Cleveland: CRC Press, **1976**, 411-422.
[27] Accelrys Software Inc., *Discovery Studio Modeling Environment, Release 3.1*, San Diego: Accelrys Software Inc., 2012.
[28] D Schneidman-Duhovny; Y Inbar; R Nussinov; HJ Wolfson. *Nucleic Acids Research*, **2005**, 33**,** W363-367.
[29] http://www.pymol.org/
[30] A Tiwari. *Insilico Biol*., **2007**, 7, 651-661.
[31] WJ Geary, *Coordination Chemistry Reviews*, **1971,** 7, 81.
[32] MF Iskander; L Ei-Syed; KZ Ismail. *Transition Met. Chem.*, **1979,** 4, 225.
[33] N Raman; JD Raja; A Sakthivel. *J. Chem. Sci.*, **2007,** 119, 303.
[34] M Thomas; MKM Nair; RK Radhakrishan. *Synth. React. Inorg. Met.-Org. Chem.*, **1995,** 25, 471-479.
[35] ABP Lever; E Mantovani. *Inorg. Chem.*, **1971,** 10, 817.
[36] ABP Lever. *Inorganic Electronic Spectroscopy*, Elsevier, New York, NY, USA, **1968.**
[37] G Maki. *J. Chem. Phys.*, **1958,** 28**,** 651.
[38] RP Ray; D Sen. *Journal of Indian Chemical Society*, **1948,** 25, 473.
[39] VK Rema Devi; A Fernandez; M Alaudeen. *Asian J. Chem.*, **2003,** 15, 1380.
[40] KG Dutton; GD Fallon; KS Murray. *Inorg. Chem.*, **1988,** 27, 34-38.
[41] M Base; K Ohta; Y Babu; MD Sastry. *Chem. Phys. Lett.*, **2000,** 324**,** 330.
[42] RK Ray; GB Kauffman. *Inorg. Chim. Acta*, **1990,** 173, 207.
[43] K Jeyasubramanian; SA Samath; S Thambidurai; R Murugesan; SK Ramalingam. *Trans. Met. Chem.*, **1996,** 20, 76.
[44] AMF Benial; V Ramakrishnan; R Murugesan. *Spectrochim. Acta, Part A*, **2000,** 56, 2775.
[45] LJ Boucher; EC Tyanan; TF Yen. *Electron Spin Resonance of Metal Chelates*,
Plenum Press, New York, **1969**.
[46] MJ Pelczar; ECS Chan; NR Krieg. '*Microbiology*', 5th Edn., Mcgraw-Hill, New Delhi **1988**.

[47] Y Anjaneyalu; RP Rao. *Synth. React. Inorg. Met.-Org. Chem.*, **1986,** 16, 257.
[48] L Mishra; VK Singh, *Indian J. Chem., Sect A,* **1993**, 32**,** 446.
[49] S Belaid; A Landreau; S Djebbar; O Benali-Baitich; G Bouet; JP Bouchara. *J. Inorg. Biochem.*, **2008,** 102, 63.
[50] N Dharamaraj; P Viswanathamurthi; K Natarajan. *Trans. Met. Chem.*, **2001,** 26, 105.